



OPEN

DATA DESCRIPTOR

VinDr-Mammo: A large-scale benchmark dataset for computer-aided diagnosis in full-field digital mammography

Hieu T. Nguyen^{1,7}, Ha Q. Nguyen^{1,2,7}, Hieu H. Pham^{1,2,3,7}✉, Khanh Lam⁴, Linh T. Le⁵, Minh Dao¹ & Van Vu^{1,6}

Mammography, or breast X-ray imaging, is the most widely used imaging modality to detect cancer and other breast diseases. Recent studies have shown that deep learning-based computer-assisted detection and diagnosis (CAdE/x) tools have been developed to support physicians and improve the accuracy of interpreting mammography. A number of large-scale mammography datasets from different populations with various associated annotations and clinical data have been introduced to study the potential of learning-based methods in the field of breast radiology. With the aim to develop more robust and more interpretable support systems in breast imaging, we introduce VinDr-Mammo, a Vietnamese dataset of digital mammography with breast-level assessment and extensive lesion-level annotations, enhancing the diversity of the publicly available mammography data. The dataset consists of 5,000 mammography exams, each of which has four standard views and is double read with disagreement (if any) being resolved by arbitration. The purpose of this dataset is to assess Breast Imaging Reporting and Data System (BI-RADS) and breast density at the individual breast level. In addition, the dataset also provides the category, location, and BI-RADS assessment of non-benign findings. We make VinDr-Mammo publicly available as a new imaging resource to promote advances in developing CAdE/x tools for mammography interpretation.

Background & Summary

Breast cancer is among the most prevalent cancers and accounts for the largest portion of cancer deaths, with an estimated 2.2 million new cases in 2020¹. Treatment is most successful when breast cancer is at its early stage. Biennial screening can reduce breast cancer mortality rate by 30%². Among standard imaging examinations for breast cancer diagnosis, namely mammography, ultrasound, digital breast tomosynthesis, and magnetic resonance, mammography is the recommended modality for cancer screening³. Interpreting mammography for breast cancer screening is a challenging task. The recall rate of mammogram screening is around 11% with a sensitivity of 86.9%, while the cancer detection rate is 5.1 per 1,000 screens⁴. It means that a large portion of cases called back for further examinations eventually result in non-cancer. Improving cancer screening results may help reduce the cost of follow-up examinations and unnecessary mental burdens on patients.

With recent advancements of learning-based algorithms for image analysis^{5,6}, several works have adapted deep learning networks for mammography interpretation and showed potential to use in clinical practices^{7–12}. In retrospective settings, the CAD tool as an independent reader can achieve a performance comparable to an average mammographer⁸. It can be leveraged as a decision support tool that helps enhance radiologists' cancer detection with the reading time being unchanged⁹. In another human-machine hybrid setting, where radiologists and machine-learning algorithm independently estimate the malignancy of the lesions, the linear combination of human and machine prediction show higher performance than a single human or machine reader¹⁰.

¹Institute of Big Data, Hanoi, Vietnam. ²College of Engineering and Computer Science (CECS), VinUniversity, Hanoi, Vietnam. ³VinUni-Illinois Smart Health Center, Hanoi, Vietnam. ⁴Hospital 108, Department of Radiology, Hanoi, Vietnam. ⁵Hanoi Medical University Hospital, Department of Radiology, Hanoi, Vietnam. ⁶Yale University, Department of Mathematics, New Heaven, CT, 06511, USA. ⁷These authors contributed equally: Hieu T. Nguyen, Ha Q. Nguyen, Hieu H. Pham. ✉e-mail: hieu.ph@vinuni.edu.vn

Dataset	Origin	Introduction year	#studies	#images	Finding type	Annotations	BI-RADS assessment	Breast density	Mode of acquisition
MIAS ¹⁹	United Kingdom	1994	161	322	Mass, calcification, asymmetry, and distortion	Circle around the finding, specified by center and radius	No	Yes	SFM
DDSM ¹⁸	United States	1999	2,620	10,480	Mass and Calcification	Contour enclosing the finding	Yes	Yes	SFM
INBreast ¹⁷	Portugal	2012	115	410	Mass, calcification, asymmetry, and distortion	Contour enclosing the finding	Yes	Yes	FFDM
NYU Dataset ¹⁶	United State	2019 [†]	229,426	1,001,093	Biopsied lesions	Contour enclosing the finding	Yes	Yes	FFDM
CSAW-CC ¹⁴	Sweden	2020	24,694	98,788	Visible tumors & tumor signs	Contour enclosing the finding	No	No	FFDM
OMI-DB ¹³	United Kingdom	2021	NA	3,072,878*	Lesions	Rectangular region of interest	No	No	FFDM
CMMD ¹⁵	China	2021	1,775	5,202	Biopsied abnormalities(mass or calcification)	No local annotations	No	No	FFDM
VinDr-Mammo	Vietnam	2022	5,000	20,000	Mass, calcification, asymmetry, distortion, and other associated features	Rectangular region of interest	Yes	Yes	FFDM

Table 1. Summary of mammography datasets. [†]Not publicly accessible *Including for-presentation and for-processing images

Annotator	Years' experience	Annual Diagnostic Volume (studies)
Radiologist 1	14	10,000
Radiologist 2	21	15,000
Radiologist 3	22	15,000
Average	19	13,333

Table 2. Characteristics of the participating radiologists. Mean annual diagnostic volumes were estimated based on the number of mammogram scans interpreting.

The improvement as a result human-machine combination is also witnessed in screening mammography interpretation¹¹. Furthermore, there was evidence that shows a machine learning model developed by training on data from a specific population (UK) can generalize and perform well on another population (US)¹².

The recent progress in the study of mammography interpretation has drawn much attention with an increasing number of mammogram datasets with various characteristics, while some datasets are publicly available to the research community, some have restricted access or are not open^{13–19} (see Table 1). Digital Database for Screening Mammography (DDSM)¹⁸ and Mammographic Image Analysis Society (MIAS) dataset¹⁹ are the two earliest public datasets that provide digitalized scans of screen-film mammograms with precise annotations of breast abnormalities. The MIAS dataset was released in 1994 with 161 studies collected in the United Kingdom while the DDSM dataset consisted of 2,620 exams collected from institutions in the United States. Compared to the former one, the DDSM dataset has a significantly larger scale and follows the BI-RADS standard. To the best of our knowledge, INbreast¹⁷, released in 2012 with 115 exams from Portugal, is the very first public dataset that provides digital mammograms with lesions annotations and overall exam assessment following the BI-RADS standard. In 2019, the NYU Breast Cancer Screening Dataset¹⁶ was introduced with 229,426 screening exams, consisting of 1,001,093 images, from 141,473 women screened at NYU Langone Health. The dataset contains breast-level cancer based on biopsy results, exam-level assessment of BI-RADS, breast density, and biopsied finding annotations. While the dataset is not public, the subsequent work¹⁰ based on this dataset showed evidence that a large-scale dataset of mammography can enable a computer-aided system that helps improve radiologist performance. At around the same time, the Cohort of Screen-Aged Women Case-Control (CSAW-CC)²⁰ was opened for evaluating AI tools for breast cancer, including 1303 cancer cases and 10,000 randomly selected controls from Karolinska University Hospital. The CSAW-CC dataset is a subset of the full CSAW dataset including women screened in the Stockholm region between 2008 and 2015. In cancer cases, visible tumors in mammography were manually annotated on a pixel level. Another large-scale dataset is the OPTIMAM mammography image database¹³ (OMI-DB) which consists of images and clinical data of 172 282 women screened and diagnosed in several institutions in the United Kingdom since 2011. To access to the OMI-DB dataset, the research group must submit an application to elaborate the scientific purpose based on the dataset which will be reviewed by the OPTINAM steering committee. In addition, the Chinese Mammography Database was recently introduced, containing 1,775 studies from several Chinese institutions. All cases have breast-level benign and malignant confirmed by biopsy, and molecular subtypes are available for 749 cases. A summary of the characteristics of these datasets is given in Table 2.

Along with the existing mammography datasets, we introduce and release the VinDr-Mammo dataset, an open-access large-scale Vietnamese dataset of full-field digital mammography consisting of 5,000 four-view

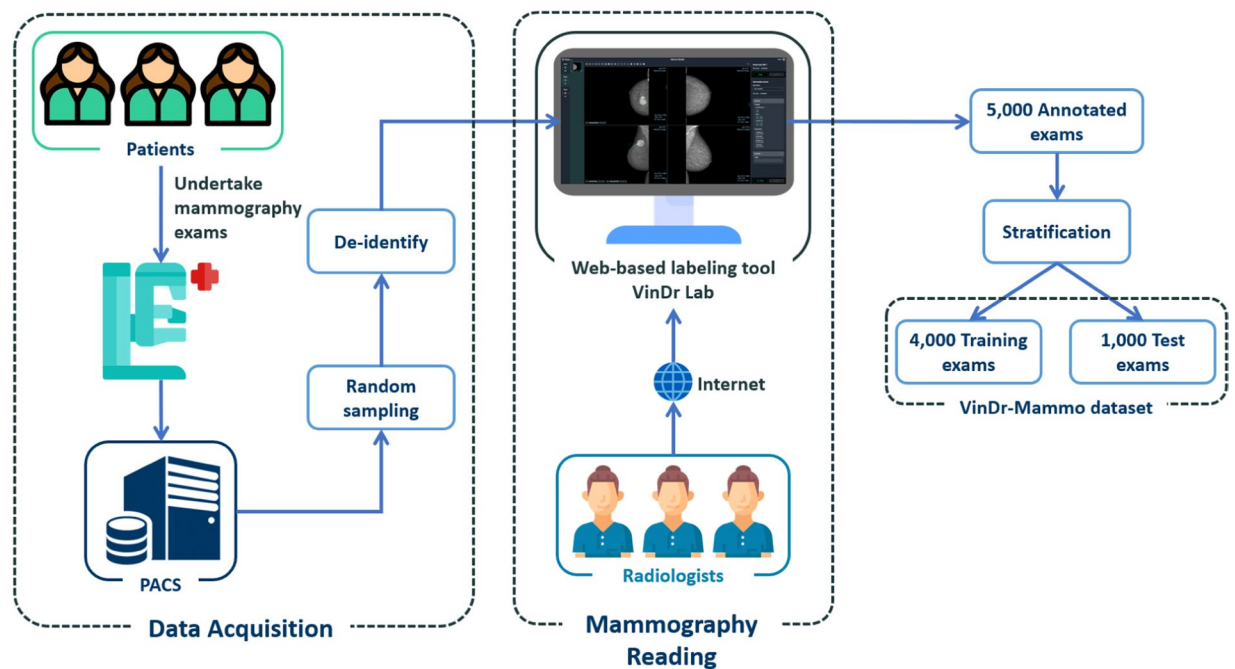


Fig. 1 Overview of the data creation process. First, for-presentation mammograms in DICOM format were collected retrospectively from the hospital's PACS. These scans then got pseudonymized to protect patient's privacy. Next, the dataset was annotated by radiologists via a web-based labeling tool called VinDr Lab, which was developed to manage medical image labeling projects with dedicated features for the medical domain. Finally, the annotated exams were split into a training set of 4,000 exams and a test set of 1,000 exams.

exams with breast-level assessment and extensive lesion-level annotations. Our aim is to enhance the diversity of the publicly available mammography data for a more robust AI system and to lean towards a more interpretable system via extensive lesion-level annotations. Mammographies were acquired retrospectively from two primary hospitals in Hanoi, Vietnam, namely Hospital 108 (H108) and Hanoi Medical University Hospital (HMHU). Breast cancer assessment and density are reported following Breast Imaging Reporting and Data System²¹. Breast abnormalities that need short-term follow-up or are suspicious of malignancy are marked by bounding rectangles. Following European guideline²², mammography exams were independently double-read. Any discordance between the two radiologists would be resolved by arbitration with the involvement of a third radiologist. To the best of our knowledge, VinDr-Mammo is currently the largest public dataset (20,000 scans) of full-field digital mammography that provides breast-level BI-RADS assessment category along with suspicious or probably benign findings that need follow-up examination. By introducing the dataset, we contribute a benchmarking imaging dataset to evaluate and compare algorithmic support systems for breast cancer screening based on FFD.

Methods

This study was approved by the Institutional Review Board of the HMUH and H108. All the personally identifiable information and protected health information of patients were removed. Additionally, this project did not affect clinical care at these two hospitals; hence patient consent was waived. The creation of the VinDr-Mammo dataset involves three stages: data acquisition, mammography reading, and data stratification. An overview of the data creation process is illustrated in Fig. 1.

Data acquisition. In this step, 20,000 mammography images in DICOM format from 5,000 mammography examinations were randomly sampled from the pool of all mammography examinations taken between 2018 and 2020 via the Picture Archiving and Communication System (PACS) of Hanoi Medical University Hospital (HMHU—<https://hmu.edu.vn/>) and Hospital 108 (H108—<https://www.benhvien108.vn/home.htm>). As the exams were randomly selected, the dataset includes both screening and diagnostic exams and represents the real distribution of patient cohorts in these hospitals. All images have the image presentation intent type of “FOR PRESENTATION” as those of for-processing were not stored by the hospitals. Images were acquired on equipments from 3 vendors, namely SIEMENS, IMS, and Planmed. All radiographers working at these hospitals were trained and certified by HMUH. To ensure patient privacy is protected, identifiable patient information in DICOM tags is fully removed via a Python script. Only necessary information used for loading and processing DICOM images and patient demographic information, i.e., age, is retained. Besides DICOM meta-data, associated information might appear in the images, such as laterality and view of the image and sometimes the patient's name. As this textual information usually appears in the corners of the image, we remove them by setting to black all pixels in a rectangle at each corner. The size of the rectangle is determined by visually inspecting a subset of the collected dataset. To validate the pseudonymization stage, both DICOM metadata and image are manually reviewed by human readers.

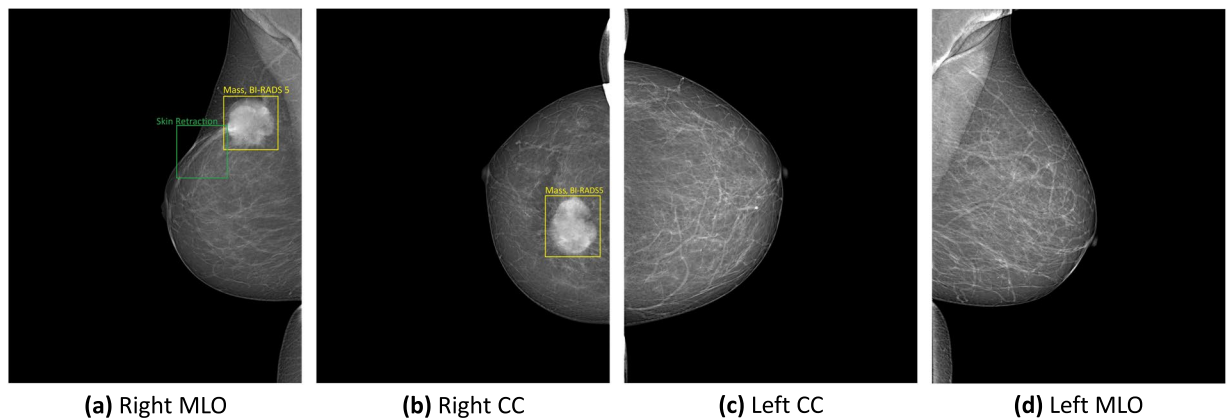


Fig. 2 A sample mammography exam with the right breast assessed with BI-RADS 5, density B and the left breast with BI-RADS 1, density B. CC denotes craniocaudal and MLO denotes mediolateral oblique.

Mammography reading. This dataset aims to provide both the overall assessment of the breast and information of local-level findings, which are essential to developing CADx and CADe systems for breast cancer screening. To this end, the 5,000 sampled exams containing 20,000 images were re-read, as the associated radiology reports do not indicate the exact locations of the findings.

The reading results follow the schema and lexicon of the Breast Imaging Reporting and Data System²¹. At the breast level, the overall BI-RADS assessment categories and breast density level (also termed breast composition) are provided. There are seven BI-RADS assessment categories, namely BI-RADS 0 (need additional imaging or prior examinations), BI-RADS 1 (negative), BI-RADS 2 (benign), BI-RADS 3 (probably benign), BI-RADS 4 (Suspicious), BI-RADS 5 (highly suggestive of malignancy) and BI-RADS 6 (known biopsy-proven). Since the biopsy results are not available, there is no presence of BI-RADS 6 in the re-reading process. Regarding the breast density level, its four categories are A (almost entirely fatty), B (scattered areas of fibroglandular), C (heterogeneously dense), and D (extremely dense). For the mammography findings, the list of findings provided in this dataset includes the mass, calcification, asymmetries, architectural distortion, and other associated features, namely suspicious lymph node, skin thickening, skin retraction, and nipple retraction. Each finding is marked by a bounding box to localize the abnormal finding. In the given finding list, BI-RADS assessment is provided for mass, calcification, asymmetries, and architectural distortion. Since the purpose of this dataset is for breast cancer screening, benign findings, i.e., findings of BI-RADS 2, are not reported to reduce the annotating time. Only findings of BI-RADS categories greater than 2, which are not confident of benign or likely to be malignant, are marked. More details of the reading reports are provided in supplementary materials. Figure 2 illustrates a sample mammography exam with both finding annotations and breast-level assessments reported by radiologists.

The mammography reading process was facilitated by a web-based annotation tool called VinDr Lab (<https://github.com/vinbigdata-medical/vindr-lab>), which was specifically designed for viewing and annotating medical images with the medical image viewer being based on the Open Health Imaging Foundation project (<https://ohif.org/>). The three participating radiologists were able to remotely access the data for reading and annotating. All three radiologists hold healthcare professional certificates, which require up to eight years of training program, and are approved by the Joint Review Committee on Education in Radiology, Vietnamese Ministry of Health. Furthermore, each reader has more than ten years of experience in the field. Specifically, all three radiologists received training in mammography interpretation and had an average of 19 years of clinical experience interpreting mammography (range 14–22 years). Additionally, each annotator reviewed an average of 13,333 mammography exams annually (range 10,000–15,000). Table 2 shows the characteristics of the radiologists who participated in our data annotation process.

Each mammography exam was then assigned to two radiologists and read independently. In cases of discordance, the exam would be assigned to the third radiologist at a higher senior experience level to make the final decision taking into account annotations of previous readers. After completing the reading process, the breast-level categories and local annotations were exported in JavaScript Object Notation (JSON) format. Subsequently, we parsed the exported file to discard unnecessary information, namely annotation timestamp, and radiologist's identifier then simplified the file's structure and transformed it to comma-separated values (CSV) file so that it could be easily parsed.

Data stratification. Recent CADx and CADe solutions are mostly learning-based approaches that require separating the dataset into disjoint subsets for training and evaluation. A pre-defined training/test split would help guarantee that different research works will use the same exams for training and testing. Otherwise, inconsistent or unstated splits in different research works might hinder the reproducibility and comparison of these works. For an appropriate stratification, both the training and test sets should reflex the assessment, composition, and distribution of findings of the whole dataset. However, stratifying that dataset while preserving the correlation between various data characteristics is challenging as the number of combinations of different attributes grows exponentially with the number of attributes (in this case BI-RADS, breast composition, and findings

	Breast BI-RADS					Total
	1	2	3	4	5	
Training	5,362 (67.03%)	1,871 (23.39%)	372 (04.65%)	305 (03.81%)	90 (01.12%)	8,000
Test	1,341 (67.05%)	467 (23.35%)	93 (04.65%)	76 (03.80%)	23 (01.15%)	2,000
Overall	6,703 (67.03%)	2,338 (23.38%)	465 (04.65%)	381 (03.81%)	113 (01.13%)	10,000

Table 3. Statistics of breast-level BI-RADS assessment.

	Breast Density				Total
	A	B	C	D	
Training	40 (00.50%)	764 (09.55%)	6,116 (76.45%)	1,080 (13.50%)	8,000
Test	10 (00.50%)	190 (09.50)	1,530 (76.50%)	270 (13.50%)	2,000
Overall	50 (00.50%)	954 (09.54%)	7,646 (76.46%)	1,350 (13.50%)	10,000

Table 4. Statistics of breast density.

Finding	Split		Total
	Training	Test	
Mass	989 (6.181)	237 (5.925)	1,226 (6.130)
Suspicious Calcification	428 (2.675)	115 (2.875)	543 (2.715)
Asymmetry	77 (0.481)	20 (0.500)	97 (0.485)
Focal Asymmetry	216 (1.350)	53 (1.325)	269 (1.345)
Global Asymmetry	20 (0.125)	6 (0.150)	26 (0.130)
Architectural Distortion	95 (0.594)	24 (0.600)	119 (0.595)
Skin Thickening	45 (0.281)	12 (0.300)	57 (0.285)
Skin Retraction	15 (0.094)	3 (0.075)	18 (0.090)
Nipple Retraction	30 (0.188)	7 (0.175)	37 (0.185)
Suspicious Lymph Node	46 (0.288)	11 (0.275)	57 (0.285)

Table 5. Findings statistics on the VinDr-Mammo dataset. The number of findings and the rate of findings per 100 images are provided for the training set, test set, and the whole dataset.

categories). Hence, we split the dataset by an algorithm called iterative stratification²³ which bases on a relaxed target that only retains a fraction of the appearance of each attribute while ignoring their co-occurrence. One-fifth of the dataset, equivalent to 1,000 exams, is for testing and the rest for training. The attributes that are taken into account for splitting include breast-level BI-RADS categories, breast composition, findings categories, and the attached BI-RADS categories (if any). The distribution of breast-level BI-RADS categories, breast composition, and findings for each subset are provided in Tables 3–5, respectively. The BI-RADS assessment of finding and patient age distribution are also depicted in Figs. 3, 4.

Data Records

Both DICOM images and radiologists' annotations of the dataset are available on PhysioNet²⁴ for public access. Breast-level and lesion-level annotations of the whole dataset are stored in CSV files `breast-level_annota-tions.csv` and `finding_annota-tions.csv`, respectively. The images are structured into subfolders according to the encoded study identifiers, each of which contains four images corresponding to four views of the exam. The subfolder name and image file name are named following the study identifier and image identifier. The information of the breast-level annotations is provided for each image even though there is redundancy since each breast is associated with two images of different view positions, i.e., MLO and CC. We find this representation more convenient because other metadata of the image, namely laterality and view position, can also be included, eliminating the need to parse this information from the DICOM tags. Metadata for each image in the `breast-level_annota-tions.csv` file includes:

- `study_id`: The encoded study identifier.
- `series_id`: The encoded series identifier.
- `image_id`: The encoded image identifier.
- `laterality`: Laterality of the breast depicted in the image. Either L or R.
- `view_position`: Breast projection. Standard views are CC and MLO.
- `height`: Height of the image.
- `width`: Width of the image.
- `breast_birads`: BI-RADS assessment of the breast that the image depicts.
- `breast_density`: Density category of the breast that the image depicts.
- `split`: Indicating the split to which the image belongs. Either `training` or `test`.

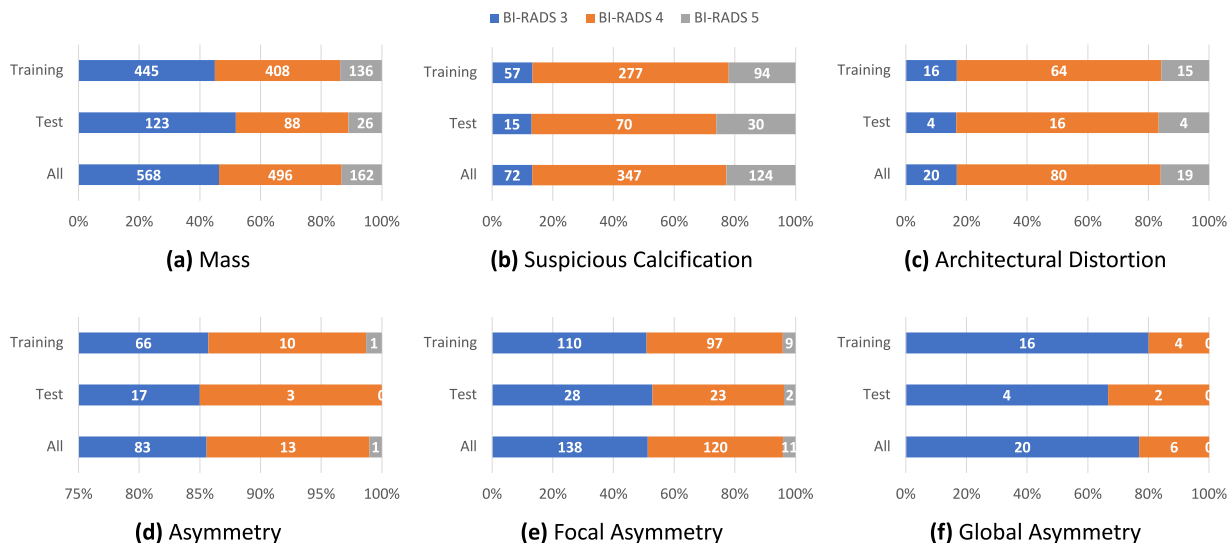


Fig. 3 Statistics of BI-RADS assessment of findings.

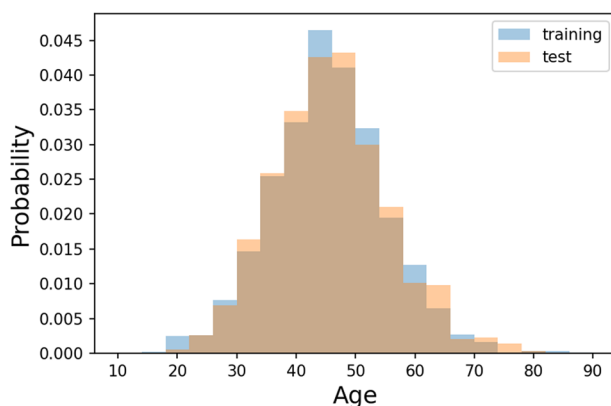


Fig. 4 Distribution of patient age. This statistic is calculated overall all exams in which patient's age is available.

Regarding breast findings, each annotation represents the occurrence of breast abnormality at a region, represented by a bounding box, in a specific image. This means that a single finding may associate with annotations from different views, yet this linking information is not acquired in the annotation process. Metadata for each finding annotation in the `finding_annotations.csv` file contains:

- `image_id`: The encoded identifier of the image in which the finding appears.
- `study_id`: The encoded identifier of the associated study.
- `series_id`: The encoded identifier of the associated series.
- `laterality`: Laterality of the breast in which the finding appears.
- `view_position`: Orientation with respect to the breast of the image.
- `height`: Height of the image.
- `width`: Width of the image.
- `breast_birads`: BI-RADS assessment of the breast that the image depicts.
- `breast_density`: Density category of the breast that the image depicts.
- `finding_categories`: List of finding categories attached to the region, e.g., mass with skin retraction.
- `finding_birads`: BI-RADS assessment of the marked finding.
- `xmin`: Left boundary of the box.
- `ymin`: Top boundary of the box.
- `xmax`: Right boundary of the box.
- `ymax`: Bottom boundary of the box.
- `split`: Indicating the split to which the image belongs. Either `training` or `test`.

Technical Validation

The data pseudonymization procedure and the quality of the labeling process were strictly controlled. First, all meta-data was manually reviewed to ensure that all individually identifiable health information or PHI²⁵ of the patients has been fully removed to meet data privacy regulations such as the U.S. HIPAA²⁶ and the European GDPR²⁷. In addition, the image content of all mammograms was manually reviewed case-by-case by human readers to ensure that no patient information remained. We developed a set of rules underlying our labeling tool to reduce mislabeling. These rules allowed us to verify the radiologist-generated labels automatically. Specifically, they prevent annotators from mechanical mistakes like forgetting to choose global labels or marking lesions on the image while choosing “BI-RADS 1” as the breast-level assessment.

Usage Notes

The VinDr-Mammo dataset was created for the purpose of developing and evaluating computer-aided detection and diagnosis algorithms based on full-field digital mammography. In addition, it can also be used for general tasks in computer vision, such as object detection and multiple-label image classification. To download and explore this dataset, users are required to accept a Data Usage Agreement (DUA) called PhysioNet Credentialed Health Data License 1.5.0 (<https://www.physionet.org/about/licenses/physionet-credentialed-health-data-license-150/>). By accepting this DUA, users agree that the dataset can be used for scientific research and educational purposes only and will not attempt to re-identify any patients, institutions or hospitals. Additionally, the authors should cite this original paper for any publication that explores this dataset.

In this study, our objective is to provide an extensive open dataset of mammograms that include annotations from radiologists. We have used the consensus among radiologists as ground truth to ensure the reliability of the annotations. However, the VinDr-Mammo dataset has certain limitations such as the absence of pathology-confirmed ground truth data and other essential clinical information like molecular and histology data. As a result, it relies heavily on the expertise of radiologists. Biopsy tests are currently the most reliable means of measuring breast cancer. However, obtaining a significant number of mammographic images, each with a biopsy test, is impractical and outside the scope of this study. Given the data's incomplete support from pathology reports, it should not be used to directly evaluate CAD for diagnosis purposes, but only used in training settings. For the screening purpose, the dataset can be directly used to evaluate CAD after converting the provided BI-RADS annotations in 5 categories to the 3-category system: BI-RAS 0 (recall, correspond to BI-RADS 3, BI-RADS 4, BI-RADS 5), BI-RAS 1 (normal, correspond to BI-RADS 1), BI-RAS 2 (benign, correspond to BI-RADS 2). Additionally, some abnormalities, such as skin and nipple retraction, have less than 40 samples, making studying these abnormalities on this dataset less reliable. Finally, the introduced dataset is not DICOM-compliant and it would fail to be processed properly by DICOM processing libraries.

Code availability

The codes used in this study were made publicly available. The scripts used for loading and processing DICOM images are based on the following open-source repositories: Python 3.8.0 (<https://www.python.org/>); Pydicom 1.2.0 (<https://pydicom.github.io/>); and Python hashlib (<https://docs.python.org/3/library/hashlib.html>). The code for data pseudonymization and stratification was made publicly available at <https://github.com/vinbigdata-medical/vindr-mammo>.

Received: 7 March 2022; Accepted: 24 March 2023;

Published online: 12 May 2023

References

- Sung, H. *et al.* Global cancer statistics 2020: Globocan estimates of incidence and mortality worldwide for 36 cancers in 185 countries. *CA: a cancer journal for clinicians* **71**, 209–249 (2021).
- Mandelblatt, J. S. *et al.* Collaborative modeling of the benefits and harms associated with different us breast cancer screening strategies. *Annals of internal medicine* **164**, 215–225 (2016).
- Siu, A. L. Screening for breast cancer: Us preventive services task force recommendation statement. *Annals of internal medicine* **164**, 279–296 (2016).
- Lehman, C. D. *et al.* National performance benchmarks for modern screening digital mammography: update from the breast cancer surveillance consortium. *Radiology* **283**, 49–58 (2017).
- Krizhevsky, A., Sutskever, I. & Hinton, G. E. Imagenet classification with deep convolutional neural networks. *Advances in neural information processing systems* **25**, 1097–1105 (2012).
- LeCun, Y., Bengio, Y. & Hinton, G. Deep learning. *Nature* **521**, 436–444 (2015).
- Dembrower, K. *et al.* Effect of artificial intelligence-based triaging of breast cancer screening mammograms on cancer detection and radiologist workload: a retrospective simulation study. *The Lancet Digital Health* **2**, e468–e474 (2020).
- Rodriguez-Ruiz, A. *et al.* Stand-alone artificial intelligence for breast cancer detection in mammography: comparison with 101 radiologists. *JNCI: Journal of the National Cancer Institute* **111**, 916–922 (2019).
- Rodriguez-Ruiz, A. *et al.* Detection of breast cancer with mammography: effect of an artificial intelligence support system. *Radiology* **290**, 305–314 (2019).
- Wu, N. *et al.* Deep neural networks improve radiologists' performance in breast cancer screening. *IEEE Transactions on Medical Imaging* **39**, 1184–1194, <https://doi.org/10.1109/TMI.2019.2945514> (2020).
- Shaffner, T. *et al.* Evaluation of Combined Artificial Intelligence and Radiologist Assessment to Interpret Screening Mammograms. *JAMA Network Open* **3**, e200265–e200265, <https://doi.org/10.1001/jamanetworkopen.2020.0265> (2020).
- McKinney, S. M. *et al.* International evaluation of an ai system for breast cancer screening. *Nature* **577**, 89–94 (2020).
- Halling-Brown, M. D. *et al.* Optimam mammography image database: a large-scale resource of mammography images and clinical data. *Radiology: Artificial Intelligence* **3**, e200103 (2021).

14. Dembrower, K., Lindholm, P. & Strand, F. A multi-million mammography image dataset and population-based screening cohort for the training and evaluation of deep neural networks—the cohort of screen-aged women (csaw). *Journal of digital imaging* **33**, 408–413 (2020).
15. Cui, C. *et al.* The chinese mammography database (cmmd): An online mammography database with biopsy confirmed types for machine diagnosis of breast. *The Cancer Imaging Archive* <https://doi.org/10.7937/tcia.eqde-4b16> (2021).
16. Wu, N. *et al.* The nyu breast cancer screening dataset v1. 0. *New York Univ., New York, NY, USA, Tech. Rep* (2019).
17. Moreira, I. C. *et al.* Inbreast: toward a full-field digital mammographic database. *Academic radiology* **19**, 236–248 (2012).
18. PUB, M. H., Bowyer, K., Kopans, D., Moore, R. & Kegelmeyer, P. The digital database for screening mammography. In *Proceedings of the Fifth International Workshop on Digital Mammography*, 212–218 (Medical Physic Publishing, 2000).
19. Suckling, J. P. The mammographic image analysis society digital mammogram database. *Digital Mammo* 375–386 (1994).
20. Strand, F. CSAW-CC (mammography). *Karolinska Institutet*. <https://doi.org/10.5878/45vm-t798> (2022).
21. Sickles, E. A. *et al.* *ACR BI-RADS® Mammography*, fifth edn (American College of Radiology, 2013).
22. Amendoeira, I. *et al.* *European guidelines for quality assurance in breast cancer screening and diagnosis* (European Commission, 2013).
23. Sechidis, K., Tsoumakas, G. & Vlahavas, I. On the stratification of multi-label data. In *Joint European Conference on Machine Learning and Knowledge Discovery in Databases*, 145–158 (Springer, 2011).
24. Pham, H. H., Trung, H. N. & Nguyen, H. Q. Vindr-mammo: A large-scale benchmark dataset for computer-aided detection and diagnosis in full-field digital mammography. *Physionet* <https://doi.org/10.13026/br2v-7517> (2022).
25. Isola, S. & Al Khalili, Y. Protected Health Information (PHI). <https://www.ncbi.nlm.nih.gov/books/NBK553131/> (2019).
26. US Department of Health and Human Services. *Summary of the HIPAA privacy rule*. <https://www.hhs.gov/hipaa/for-professionals/privacy/laws-regulations/index.html> (2003).
27. European Parliament and Council of European Union. Regulation (EU) 2016/679 (General Data Protection Regulation). <https://gdpr-info.eu/>. (Online; accessed 11 December 2020) (2016).

Acknowledgements

We would like to acknowledge the Hanoi Medical University Hospital and Hospital 108 for their collaboration in creating the VinDr-Mammo dataset and for agreeing to make it publicly available. We are especially thankful to the radiologist team Nhung Hong Luu, Minh Thi Ngoc Nguyen, Huong Thu Lai, and other collaborators who participated in the data collection and labeling process.

Author contributions

H.Q.N. and H.H.P. designed the study; H.T.N. performed the data pseudonymization and data stratification; H.H.P. and H.T.N. conducted the data acquisition and analysis; H.H.P. and H.T.N. wrote the paper; all authors reviewed the manuscript.

Competing interests

This work was funded by the Vingroup JSC. The funder had no role in study design, data collection, and analysis, decision to publish, or preparation of the manuscript.

Additional information

Supplementary information The online version contains supplementary material available at <https://doi.org/10.1038/s41597-023-02100-7>.

Correspondence and requests for materials should be addressed to H.H.P.

Reprints and permissions information is available at www.nature.com/reprints.

Publisher's note Springer Nature remains neutral with regard to jurisdictional claims in published maps and institutional affiliations.



Open Access This article is licensed under a Creative Commons Attribution 4.0 International License, which permits use, sharing, adaptation, distribution and reproduction in any medium or format, as long as you give appropriate credit to the original author(s) and the source, provide a link to the Creative Commons license, and indicate if changes were made. The images or other third party material in this article are included in the article's Creative Commons license, unless indicated otherwise in a credit line to the material. If material is not included in the article's Creative Commons license and your intended use is not permitted by statutory regulation or exceeds the permitted use, you will need to obtain permission directly from the copyright holder. To view a copy of this license, visit <http://creativecommons.org/licenses/by/4.0/>.

© The Author(s) 2023